brief communication

Monomer diffusion into polymer domains in sickle hemoglobin

Michael R. Cho and Frank A. Ferrone
Department of Physics and Atmospheric Science, Drexel University, Philadelphia, Pennsylvania 19104 USA

ABSTRACT The gelation of sickle hemoglobin includes the formation of spherulitic arrays of polymers, known as polymer domains, which are an intrinsic result of the polymer formation mechanism. We have observed the diffusion of monomers into domains as they form, which substantially increases the total concentration of hemoglobin within the domain. The maximum total concentration attained is comparable with the pellet concentration of 0.5–0.55 g/cm^3 obtained in sedimentation experiments. The half time for this process is ~50 s for domains of 25 μm radius, and is approximately independent of temperature. The shape of the diffusion progress curves as well as the deduced diffusion constants, and their weak temperature dependence are consistent with a simple model of hemoglobin monomer diffusion into the domain.

INTRODUCTION

The gelation of sickle hemoglobin is a multifaceted process, involving homogeneous nucleation of polymers in bulk solution, the heterogeneous nucleation of polymers onto other polymers, and the alignment of the polymers into spherulitic domains (Eaton and Hofrichter, 1987; Basak et al., 1988; Ferrone, 1989). The effects of solution nonideality and the large size of the homogeneous and heterogeneous nuclei endow the process of gelation with a strong concentration dependence, that itself depends upon concentration (Ferrone et al., 1985*a* and *b*).

Domains of aligned polymers were long observed (Hofrichter, 1979; Hofrichter et al., 1976*a*; White and Heagan, 1970) before their relationship to the mechanism of polymer formation emerged because alignment could well be controlled by factors wholly different from those that govern the nucleation and growth processes. The integral role of domains was established principally as the result of experiments in which the delay time became stochastically variable while the subsequent growth reproducibly formed a single, aligned domain (Ferrone et al., 1980; Ferrone et al., 1985*a* and *b*; Hofrichter, 1986). This implied that one polymer gave rise to many, thus, connecting domains with the mechanism. In experiments that spatially resolved the growth of domains, polymers were clearly seen to grow in expanding arrays. This observation was qualitatively in keeping with the double nucleation mechanism, because the ability of a given polymer to nucleate additional polymers confers a spatial dimension on the reaction (Basak et al., 1988; Ferrone, 1989). Recently we have shown that the spatially resolved observations are also quantitatively consistent with the double nucleation model (Zhou and Ferrone, 1990).

A consequence of the spatial nonuniformity of the reaction is that monomers are expected to diffuse into a polymer domain as the initial monomer concentration is diminished, due to the differential mobility of monomers and polymers. *A priori,* neither the extent nor the timescales of such diffusion are evident. Whereas there has been some evidence for diffusion in spatially integrated experiments, the effect can easily be masked without explicit spatial resolution because the spatially averaged quantity is intensity, rather than optical density. Thus, we have sought to determine how much monomer diffusion will occur, and how rapidly this process happens. We report here the initial findings of experiments designed to probe this feature of gelation.

METHODS

The experiments used a microscopic photolysis technique with a focused steady-state laser to create and maintain deoxyhemoglobin in a small region of a 4–6 μm thick carboxyhemoglobin sample, which covered ~3 cm^2 area (Basak et al., 1988). The laser was typically focused into an ellipse of major diameters 48 × 44 μm. A two-dimensional 50 × 50 μm image ("frame") of that region of the sample is collected by a silicon-intensified target vidicon. The spatial and temporal growth of polymer domains are followed by interleaving light scattering and absorbance frames. Scattering, measured at 514 nm, located the domain center and triggered data collection when scattering exceeds 6% of the background. Thereafter, the absorbance increase was used to trigger each subsequent frame of data collection. When an absorbance frame was collected, a corresponding scattering frame was recorded 3 s later. This process continued until the computer memory was filled.

Absorbance was measured at 430 nm, which responds to the concentration of deoxyhemoglobin, regardless of state of polymerization. Control absorbance experiments performed at 420 nm gave comparable results. Experiments at 488 nm showed no absorbance change, eliminating turbidity as a possible cause of transmission loss. Most of the

0006-3495/90/10/1067/07 $2.00

experiments reported (except as specifically noted) were performed with parallel polarizers located before and after the sample, oriented vertically or horizontally. In a few experiments, the absorbance beam was almost unpolarized, i.e., the polarization in two orthogonal directions differed by no more than 20%. At the termination of every experiment, crossed polarizers were inserted before and after the sample, and its birefringence was observed at 488 nm. The appearance of a characteristic "Maltese Cross" pattern was used to confirm that only one domain had formed. Other aspects of the experiment are described by Basak et al. (1988).

RESULTS

Fig. 1 shows absorbance and scattering contour maps for a single-growing domain viewed in unpolarized light. At time zero the argon laser hits and completely desaturates most of the sample viewed in the frame. A delay follows, composed of a stochastically variable time during which the first homogeneous nucleus forms, followed by an incubation time during which heterogeneous nucleation and polymer growth, though present, are undetected. The exponential nature of the growth curve causes the polymers to appear quite abruptly. Thereafter, scattering and absorbance frames are alternately collected. The outer–absorbance contours are set by the desaturation produced by the laser beam, and remain essentially constant. In contrast, the inner contours grow in height and extent as hemoglobin diffuses into the domain. The scattering begins in a small region and spreads outward. At the center, scattering reaches a maximum and decreases, while absorbance continues to rise. At longer times the peak absorbance has nearly saturated and the approximate radial symmetry of the absorbance increase breaks down into an elongated pattern, which depends on the polarization of the input beam. In experiments with a fixed, single polarization, the elongation was rotated if the polarization state was rotated. This will be discussed below. The scattering reaches a maximum early in the experiment and subsequently declines to little more than the initial scattering intensity, despite the presence of a high density of polymers. Birefringence shows a distinct cross, confirming that only one domain has formed.

To simplify the analysis, we have limited our study to single domains formed reasonably–well centered in the frame. Stochastic nucleation makes it possible to have either single or multiple domains form in the frame under the same conditions. Experiments in which more than one nucleus formed, or in which the nucleation occurred near an edge, were generally aborted. In a few experiments, which will not be discussed further in this paper, we monitored the concentration increase where multiple domains (unresolved when viewed in birefringence) had formed. These also showed a similarly large increment in concentration.

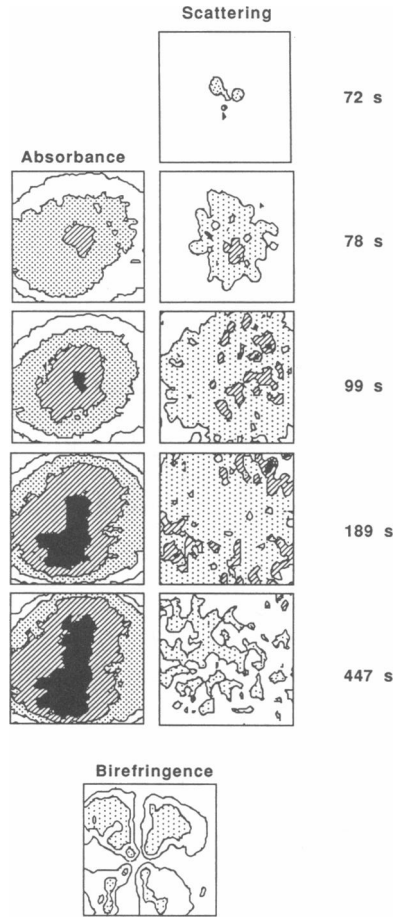

FIGURE 1 Absorbance and corresponding scattering contours describing evolution of diffusion of deoxyhemoglobin monomers into a polymer domain for a 50 × 50 μm area. Absorbance contour increments are 0.12 optical density (OD) or 0.037 g/ml of HbS monomers starting at 0.55 OD. The initial concentration of 0.335 g/ml corresponds to 0.67 OD. Diffusion of CO slightly enhances the size of the photolyzed region. Light scattering is monitored to trigger data collection. After each absorbance frame, a scattering frame was recorded 3 s later. The scale of scattering contours is arbitrary. Only 10 of the 23 frames typically collected are shown here. Birefringence is observed at 488 nm by manually inserting crossed polarizers. The logarithm of birefringence intensity is plotted to better simulate the pattern seen by eye. The sample temperature was 22.8°C.

The fact that sickle hemoglobin polymers are not optically isotropic will create difficulties in interpretation if the fibers are aligned. The alignment gives rise to the well-known linear dichroism and birefringence. The effect of the alignment is to decrease the measured optical density for a given polymer concentration. If we denote as ϵ_0 the extinction coefficient of the hemoglobin monomer isotropically averaged in solution, then the extinction coefficient for light polarized parallel to the fiber is 0.34 ϵ_0 whereas perpendicular to the fiber the extinction is

greater, being 1.33 ϵ_0 (Eaton and Hofrichter, 1981). The presence of the lesser extinction coefficient in an unpolarized beam acts as a "light leak" and diminishes the absorbance. With a polarized beam, the result depends critically on whether the alignment is parallel or perpendicular to the polarizer axes. Thus, the formation of polymer domains can lead to a decrease in absorbance, due to aligned regions of anisotropic polymers, as well as an increase in absorbance due to diffusion of monomers. These effects are coupled because polymer formation drives the diffusion process.

The anisotropy that emerges in the absorbance contours (Fig. 1) is the consequence of the alignment of the polymers and a weakly polarized beam. The excess concentration will accordingly be more extensive than indicated by the optical density contours, due to the polymer alignment that is evident when the birefringence is viewed.

At the center of the cross pattern there is no birefringence. Therefore, to measure the maximum concentration of hemoglobin which diffused into the domain, a 3-μm circle was averaged at the center of cross pattern determined from the birefringence frame. There is still some ambiguity because the lack of birefringence can result from isotropically ordered polymers, or polymers randomly arrayed in the plane of the sample. These two limits bound the extinction coefficients appropriate to the problem: isotropically, the effective extinction coefficient ϵ_{eff} is just that of the monomers ϵ_0; while planar-random polymers have an extinction coefficient $\epsilon_{eff} = 0.86\ \epsilon_0$. In our analysis we will first use isotropic coefficients, and then discuss their modification.

Fig. 2 shows a typical progress curve for a 0.335 g/ml sample. Isotropic extinction coefficients have been used to generate a concentration from measured optical density. The time marked zero on the curve corresponds to the start of data collection, 570 s after initiation of laser photolysis. Whereas there is a substantial increase in the first 50 s shown, the concentration continues to rise slowly over the next 500 s. The slow increase of the curve presents an experimental problem of extrapolating to the maximum in a systematic way. We adopted an approach motivated by a simple diffusion model in which the domain represents a cylindrical hole, into which monomers diffuse. This gives a simple equation (Crank, 1975) for the excess concentration at the center of the "hole," viz.

$$c_+(t) = c_+(\infty) \exp(-a^2/4Dt) = c_+(\infty) \exp(-\tau/t) \quad (1)$$

where D is the diffusion constant, a is the radius of the cylinder (domain), $c_+(\infty)$ is the initial "depth" of the hole,

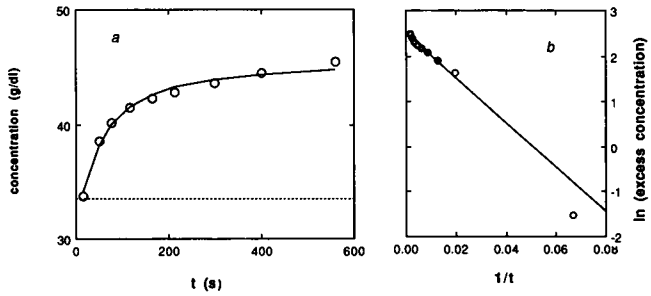

FIGURE 2 (*a*) Progress curve of the increase in concentration averaged over a circle of 3 μm radius placed at the domain center. The dashed line shows the initial sample concentration, 33.5 g/dl. Concentration was determined by using isotropic extinction coefficients. Sample temperature was 18.1°C. The domain formed 12 μm from an edge. The delay time (before zero on the graph) is 570 s. The solid curve is a fit as constructed from *b*. (*b*) The logarithm of the excess concentration as a function of $1/t$. The excess is computed as the concentration at a given time minus the initial concentration. The line is fit to the points larger than half the total increase, which are shown as the bold circles. The fit gives a characteristic time τ of 49.4 s. The intercept, giving the extrapolated maximum, is 12.3 g/dl.

and where we have defined τ as $a^2/4D$. Clearly $c_+(\infty)$ will be the maximum concentration of the diffused species c_+.

Whereas this is enormously oversimplified for the problem at hand because the domain is growing as the monomers are diffusing, it might represent a reasonable approach for the final stages of diffusion, where the domain size is circumscribed by the laser. A linear form of Eq. 1 can be obtained by plotting the log of excess concentration versus $1/t$. Plotting the data versus $1/t$ is especially useful for generating an asymptotic value and is insensitive to error in the choice of the starting time. Because this model is likely to be most accurate near the end of the diffusion process, we restricted the fit to points whose concentrations were greater than half of the final concentration. Fig. 2 *b* shows the result of this procedure. As can be seen, it produces a good fit to the tail of the curve, and is even fairly good at describing the initial part of the curve. Whereas the fit is not perfect, the deviations do not show systematic behavior over the entire data set. For example, the curve lies lower than the uppermost point in this set, and in six other sets, but lies above the final data point in five data sets.

A set of experiments were conducted at an initial concentration c_0 of 0.335 g/ml as a function of temperature over the range 10–30°C, and the results were analyzed according to the above procedure. The maximum concentration ($c_{max} = c_+(\infty) + c_0$) is shown in Fig. 3. The possibility that the polymers lie primarily in the sample plane (so that $\epsilon_{eff} = 0.86\ \epsilon_0$) is represented by the error bars. In that case, the maximum absorbance is the result of diffusion, which increases absorbance, and

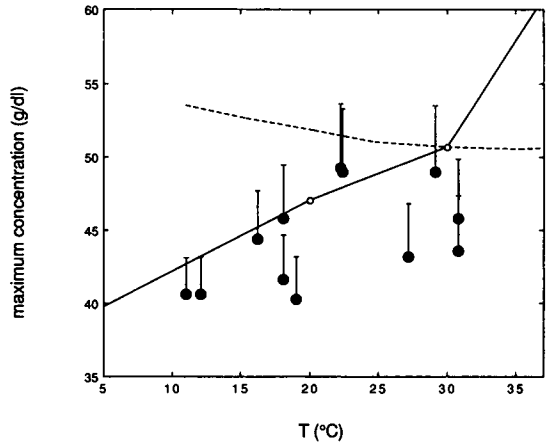

FIGURE 3 Maximum concentration as a function of temperature for initial concentration of 33.5 g/dl. The error bars extended upward by 14% of the polymer concentration, computed as the difference between the measured concentration and the solubility. This represents the increase in the concentration expected if the polymers lie randomly in the plane of the sample, rather than randomly in all directions. The solid line connects the points (*open symbols*) taken from Prouty et al. (1985). The dashed line is drawn from the solubility and the use of Eq. 2.

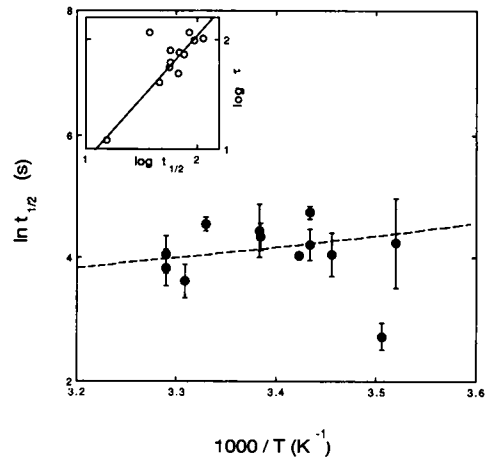

FIGURE 4 Arrhenius plot of the half time for diffusion progress curves. All samples had initial concentration of 33.5 g/dl. (*Inset*) Correlation between the half time and the characteristic times τ as determined by fitting a simple diffusion model from Eq. 1 (cf. Fig. 2) The correlation between the two procedures suggests that all the curves have the same shape. Note that the inset is in common logarithms. The line is drawn with unit slope. A best fit to all the points gives a slope of 0.96, excluding the uppermost outlier which gives a slope of 1.14.

polymer alignment in the sample plane, which decreases the absorbance. Hence, the excess concentration may need correction (i.e., error bars) to the extent that the absorbance has been diminished due to the concentration of aligned polymers. For generating such an error estimate, we assume that the final monomer concentration is just the solubility, so that the maximum polymer concentration $\Delta_{max} = c_{max} - c_s$. The errors shown in Fig. 3 are drawn as a 14% increase of Δ_{max}.

To characterize the kinetics, the half time was determined as the time between the light scattering trigger and the time for the absorbance curve to reach half its maximum. The half time for the rise in concentration is shown in Fig. 4. There is little, if any, temperature dependence, with most of the experiments showing ~50 s half time. In some experiments, the rise in absorbance is immediate, whereas in others it is slightly delayed, most likely indicating an early light scattering trigger. This can happen because of fluctuations in light scattering intensity in which a small excess above background will cause the trigger signal. Thus, the difference in time between the light scattering trigger and the point where the concentration curve rises off the time axis (cf. Fig. 2) was taken as a measure of the error in the half time and is drawn in Fig. 4 as the error bars.

The inset to Fig. 4 compares the half time with the characteristic time τ determined from Eq. 1 These two times are highly correlated. This implies that there is but a single characteristic time describing the curves, i.e., that all have essentially the same shape.

DISCUSSION

The increase in concentration of hemoglobin in the center of the polymer domain is easily understood because hemoglobin in polymers will be relatively immobile compared with the monomers. Hence, the monomers in the domain, which are consumed in producing polymers, are replenished by the diffusion of monomers from outside the domain.

The magnitude of the concentration spontaneously achieved in the domain center is comparable with packed hemoglobin polymer pellet concentration of 0.50–0.55 g/ml obtained in centrifugation experiments (Hofrichter et al., 1976*b*; Sunshine et al., 1979) in which the concentration of supernatant and volume fraction of pellet phase were measured. The maximum total concentration in those experiments was empirically described by the equation

$$c_{max} = v_{pp} c_{pp} + (1 - v_{pp}) c_s, \qquad (2)$$

in which the volume fraction occupied by polymers, v_{pp}, and the concentration of the polymer phase, c_{pp}, were taken as constants. This can be compared with our results in Fig. 3. The temperature dependence of the solubility produces a weak temperature dependence to the total concentration. Whereas there is some agreement, it is clear that the data presented here cannot be accommodated by Eq. 2 at the lower temperatures. Because Eq. 2

describes a packed-polymer phase, the disagreement is not completely surprising. In terms of the empirical parameters, the disagreement could result if the volume of the polymer phase is not a constant, for example, but increases with temperature. In the data of Sunshine et al. (1979), the choice of temperature and initial concentration to retain accessible delay times could have suppressed a variation in v_{pp}.

Osmotic stress measurements provide another means to ascertain the total concentration of hemoglobin S at a given temperature and initial concentration. The data of Prouty et al., (1985) for a 0.335 g/ml sample is shown in Fig. 3 as open symbols connected by a solid line. Agreement with our data is much better in this case, and appears to be within the relative uncertainty of the two experiments. In this context, the concentration points, which lie below the line, may be due to error in extrapolation to equilibrium. The general agreement, however, does suggest that our method produces results close to equilibrium.

The shape of the diffusion progress curves is described remarkably well by the simple model of Eq. 1. The characteristic times τ and half times also show the expected weak temperature dependence characteristic of diffusion. The dashed line in Fig. 4 shows the expected temperature dependence of the diffusion constant. This is obtained from the temperature dependence of the viscosity of water, which is related to the diffusion coefficient by $\tau \propto 1/D \propto \eta(T)/T$. The diffusion coefficient of HbS has previously been found to conform to this temperature dependence (Kam and Hofrichter, 1986). Thus, we conclude that the temperature dependence of the characteristic times is consistent with the temperature dependence expected based on pure diffusion.

From the characteristic times (cf. Eq. 1) it is possible to compute a diffusion coefficient. The average characteristic time was 34 ± 11 s, averaging the data points for all temperatures with the exception of one outlier. If the domain radius is taken as the beam radius, viz. 25 μm, the diffusion constant is calculated to be 4.6 ± 1.5 $\mu m^2/s$. By inelastic light scattering, the mutual diffusion constant for solutions of this concentration of hemoglobin has been determined to be 45–53 $\mu m^2/s$ (Jones and Johnson, 1978; Hall et al., 1980; Kam and Hofrichter, 1986). The presence of a large amount of polymer, ~65% of the volume, is likely to provide an obstruction to free diffusion into the domain. The diffusion equation for this case is not easily solved. An approximation using randomly placed obstructions, albeit for a single direction of diffusion, is described by Crank (1975), and predicts a value which is 0.27 that of free diffusion, which gives 12–14 $\mu m^2/s$ for the case here. In their study of the inelastic scattering in hemoglobin gels, Kam and Hofrichter (1986) found no decrease in the diffusion constant of monomers upon gelation, which they interpreted as the result of densely packed polymers and regions of completely mobile monomers. The present results do not dispute this interpretation, for as Kam and Hofrichter point out, the regions of mobile polymers need only be larger than the reciprocal scattering vector, i.e., >200 nm. Diffusion into the polymer domain may well be the passage of monomers between relatively free pockets with small regions of connectivity. Whereas these diffusion constants do not agree closely, we would view their similarity as a positive result given the difficulty of predicting diffusion in the domain. Thus, the time dependence, temperature dependence, and to a lesser extent, the magnitude of the characteristic time all suggest the basic correctness of a simple diffusion model. Although this description of monomer diffusion through a preformed polymer lattice is clearly oversimplified, its success in describing the diffusion seen here should be helpful in constructing a theoretical description of this generally complex phenomenon. The formulation of a more complete theory must also include that fact that the domain is not formed at precisely the beam center. Having the center closer to a free boundary would clearly improve the agreement of the expected diffusion constants, for example.

If diffusion is relatively rapid, then replacement of the monomers consumed in polymer formation is virtually instantaneous; if diffusion is slow, the external monomers may have replaced only some of the polymerized monomers. However, there is no way in which more hemoglobin can diffuse into the domain than that immobilized as polymers. The excess hemoglobin concentration, therefore, sets a lower limit to the concentration of monomers "lost" to polymers.

It is interesting to compare the light scattering signal, which has been extensively used to characterize the reaction, with the monomer diffusion. Although it has been observed that the light scattering will eventually decrease after reaching its maximum, it is unknown at what point the signal may no longer be regarded as proportional to the polymer mass. Previously (Ferrone et al., 1985*b*) the peak scattering was set equal to the maximum expected polymer concentration, $c_0 - c_s$. If the excess concentration exactly matches the polymerized hemoglobin, then the earliest excess concentration point can be equated to the scattering, which occurs at the same time. In Fig. 5 the light scattering data has been scaled so that the first point of light scattering is set equal to the excess monomer concentration for the same time. When this is done, subsequent scattering points exceed the expected concentration curve before the peak is reached. If the polymerized hemoglobin exceeds the excess concentration at the time of the first point, then the scattering should accordingly exceed the absorbance there. In either case, it is clear that the light scattering increases more

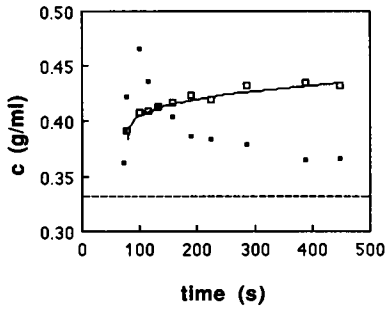

FIGURE 5 Comparison of progress curves of scattering (*solid squares*) and the increase of total HbS concentration (*open squares*). The initial concentration is shown as the dotted line. The data is from the experiment of Fig. 1. Initial scattering and absorbance points have been set equal.

rapidly than the polymer mass, before the scattering signal decreases.

The pathophysiological implications of diffusion processes observed here bear discussion because a number of key elements are different in vivo. In our experiments, there is almost 1,000 times as much hemoglobin in the sample as in the domain under study, providing a reservoir for diffusion. Because a red cell has a finite volume, a domain can scarcely be expected to concentrate to the large values seen here. However, the effect of diffusion will be to change the concentration at the domain center so as to exceed what might have been otherwise expected. In the absence of diffusion a red cell would produce a gel, which had a homogeneous polymer concentration, given by $c_0 - c_s$. However, as a domain begins to form, diffusion will transport monomers from the outside to the center. Whereas the monomer concentration at the domain periphery cannot fall below c_s, the polymer concentration at the domain center can certainly exceed $c_0 - c_s$. Thus, diffusion provides a means for mass transport, and the beginning of a phase separation. This could well have implications for the deformability of the cell. The difference in polymer density between domain center and periphery can change the deformability of the domain because viscosity depends on at least the cube of concentration of the polymerized monomers (Doi and Edwards, 1986).

It is clearly crucial to this argument that diffusion occurs at rates that exceed domain expansion. Whereas diffusion as seen here occurring at times of 50 s or more might seem too slow for physiological relevance, the diffusion time has an r^2 dependence. Thus, a domain 10 times smaller could show substantial diffusion in less than a second. Moreover, direct measurements by Briehl and co-workers (Samuel et al., 1990) as well as analysis of stochastic progress curves (Hofrichter, 1986) or of domain growth (Zhou and Ferrone, 1990) indicate that polymer growth is considerably slower than the diffusion controlled rates once thought to apply (Ferrone et al., 1985*b*). As an illustration, consider growth and diffusion in a 0.335 g/ml cell. Using the rates from Samuel et al. (1990), a polymer could have only grown 0.07 μm in 0.01 s, and accordingly a domain will have a radius smaller than this. However, taking the diffusion length as $2\sqrt{Dt}$, monomers can diffuse 0.42 μm (using the diffusion constants of this paper). At ~0.1 s, or 0.7 μm, the two processes are comparable, whereas for longer times and larger domains growth is faster. This may accordingly allow multiple growing domains to sweep out monomer concentration between them. Furthermore, the higher concentrations generated by diffusion will affect the ease with which polymers melt upon oxygen exposure (Gill et al., 1979; Gill et al., 1980; Sunshine et al., 1982).

This gives domain number and structure a role in the pathophysiology by acting as a hidden variable for the viscosity, deformability and the kinetic behavior of the cell, in a way which may permit less concentrated cells to behave as more concentrated ones. And of course, the exquisite sensitivity of gelation kinetics to monomer concentration may make these concentration-changing processes even more significant. Experiments are presently underway to follow the diffusion seen here in a more physiological setting.

We are indebted to Dr. James Hofrichter for several helpful comments and to Dr. J. T. Wang for his assistance in the initial phases of this study.

We also acknowledge the support of the Heart, Lung and Blood Institute of the National Institute of Health through grant HL28102.

Received for publication 3 October 1989 and in final form 11 July 1990.

REFERENCES

Basak, S., F. A. Ferrone, and J. T. Wang. 1988. Kinetics of domain formation by sickle hemoglobin polymers. *Biophys. J.* 54:829–843.

Crank, J. 1975. The Mathematics of Diffusion. 2nd ed. Clarendon Press, Oxford.

Doi, M., and S. F. Edwards. 1986. The theory of polymer dynamics. Oxford University Press, New York.

Eaton, W. A., and J. Hofrichter. 1981. Optical spectroscopy of hemoglobin. *Methods Enzymol.* 76:175–261.

Eaton, W. A., and J. Hofrichter. 1987. Hemoglobin S gelation and sickle cell disease. *Blood.* 70:1245–1266.

Ferrone, F. A. 1989. Kinetic models and the pathophysiology of sickle cell disease. *Ann. NY Acad. Sci.* 565:63–74.

Ferrone, F. A., J. Hofrichter, H. Sunshine, and W. A. Eaton. 1980. Kinetic studies on photolysis-induced gelation of sickle cell hemoglobin suggest a new mechanism. *Biophys. J.* 32:361–377.

Ferrone, F. A., J. Hofrichter, and W. A. Eaton. 1985*a*. Kinetics of sickle hemoglobin polymerization II: a double nucleation mechanism. *J. Mol. Biol.* 183:611–631.

Ferrone, F. A., J. Hofrichter, and W. A. Eaton. 1985*b*. Kinetics of sickle hemoglobin polymerization I: studies using temperature-jump and laser photolysis techniques. *J. Mol. Biol.* 183:591–610.

Gill, S., R. C. Benedict, L. Fall, R. Spokane, and J. Wyman. 1979. Oxygen binding to sickle cell hemoglobin. *J. Mol. Biol.* 130:175–189.

Gill, S., R. Spokane, R. C. Benedict, L. Fall, and J. Wyman. 1980. *J. Mol. Biol.* 140:299–312.

Hall, R. S., Y. S. Oh, and C. S. Johnson, Jr. 1980. Photon correlation spectroscopy in strongly absorbing and concentrated samples with applications to unliganded hemoglobin. *J. Phys. Chem.* 84:756–767.

Hofrichter, J. 1979. Ligand binding and the gelation of sickle cell hemoglobin. *J. Mol. Biol.* 128:335–369.

Hofrichter, J. 1986. Kinetics of sickle hemoglobin polymerization III. Nucleation rates determined from stochastic fluctuations in polymerization progress curves. *J. Mol. Biol.* 189:553–571.

Hofrichter, J., P. D. Ross, and W. A. Eaton. 1976*a*. A physical description of hemoglobin S gelation. *In* Proceedings of the Symposium on Molecular and Cellular Aspects of Sickle Cell Disease. J. I. Hercules, G. L. Cottam, M. R. Waterman and A. N. Schechter, editors. Department of Health, Education and Welfare, Washington, DC. Publication NIH 76–1007:185–224.

Hofrichter, J., P. D. Ross, and W. A. Eaton. 1976*b*. Supersaturation in sickle cell hemoglobin solutions. *Proc. Natl. Acad. Sci. USA.* 73:3035–3039.

Jones, C. R., and C. S. Johnson, Jr. 1978. Photon correlation spectroscopy of hemoglobin: diffusion of oxy-HbA and oxy-HbS. *Biopolymers.* 17:1581–1593.

Kam, Z., and J. Hofrichter. 1986. Quasi-elastic laser light scattering from solutions and gels of hemoglobin S. *Biophys. J.* 50:1015–1020.

Prouty, M. S., A. N. Schechter, and V. A. Parsegian. 1985. Chemical potential measurements of deoxyhemoglobin S polymerization. *J. Mol. Biol.* 184:517–528.

Samuel, R. E., E. D. Salmon, and R. W. Briehl. 1990. Direct observation of nucleation, growth and gelation of sickle cell hemoglobin (HbS) by video enhanced differential interference contrast (DIC) microscopy. *Biophys. J.* 57:229a. (Abstr.)

Sunshine, H. R., J. Hofrichter, and W. A. Eaton. 1979. Gelation of sickle cell hemoglobin in mixtures with normal adult and fetal hemoglobins. *J. Mol. Biol.* 133:435–467.

Sunshine, H. R., J. Hofrichter, F. A. Ferrone, and W. A. Eaton. 1982. Oxygen binding by sickle cell hemoglobin polymers. *J. Mol. Biol.* 158:251–273.

White, J. G., and B. Heagan. 1970. The fine structure of cell free sickled hemoglobin. *Am. J. Pathol.* 58:1–17.

Zhou, H. X., and F. A. Ferrone. 1990. A theoretical description of the spatial dependence of sickle hemoglobin polymerization. *Biophys. J.* 58:695–703.